Design of ionic liquid like monomers towards easy-accessible single-ion conductor polyelectrolytes

Luca Porcarelli[a,b,*], Petr S. Vlasov[c], Denis O. Ponkratov[d], Elena I. Lozinskaya[d], Dmitrii Y. Antonov[d], Jijeesh R. Nair[b,e], Claudio Gerbaldi[b], David Mecerreyes[a] and Alexander S. Shaplov[d,f,*]

[a]*POLYMAT, University of the Basque Country UPV/EHU, Joxe Mari Korta Center, Avda. Tolosa 72, 20018 Donostia-San Sebastian, Spain*

[b]*GAME Lab, Department of Applied Science and Technology (DISAT), Politecnico di Torino, Corso Duca degli Abruzzi 24, 10129, Torino, Italy*

[c]*Department of Macromolecular Chemistry, Saint-Petersburg State University, Universitetsky pr. 26, Saint-Petersburg, 198504, Russia*

[d]*A.N. Nesmeyanov Institute of Organoelement Compounds Russian Academy of Sciences (INEOS RAS), Vavilov str. 28, 119991 Moscow, Russia*

[e]*Helmholtz-Institute Münster (HI MS) IEK-12: Ionics in Energy Storage, Corrensstraße 46, 48149 Münster, Germany*

[f]*Luxembourg Institute of Science and Technology (LIST), 5 avenue des Hauts-Fourneaux, L-4362 Esch-sur-Alzette, Luxembourg*

*Corresponding authors: luca_porcarelli001@ehu.es, alexander.shaplov@list.lu

ABSTRACT: As the focus on developing new polymer electrolytes continues to intensify in the area of alternative energy conversion and storage devices, the rational design of polyelectrolytes with high single ion transport rates has emerged as a primary strategy for enhancing device performance. With the aim to increase ionic conductivity of single ion polymer conductors, four novel ionic liquid like monomers have been designed and synthesized in high purity. Such monomers differ from the previously published ones by the presence of long and flexible spacer between methacrylate reactive group and chemically bonded anion or by plasticizing side perfluorinated chain. The investigation of their free radical copolymerization with poly(ethylene glycol) methyl

ether methacrylate (PEGM) allowed to identify the impact of the copolymer's composition on thermal and ion conducting properties of polyelectrolytes. At that, the highest ionic conductivity (1.9×10^{-6} and 2×10^{-5} S/cm at 25 and 70 °C, respectively) was showed by the copolymer based on lithium 3-[4-(2-(methacryloyloxy)ethoxy)-4-oxobutanoyl)oxy) propylsulfonyl]-1-(trifluorometha-nesulfonyl)imide and obtained at [EO]/[Li]=61 ratio. Owing to wide electrochemical stability (4.2 V *vs.* Li^+/Li) and high lithium-ion transference number (0.91) the prepared copolymer was further applied as a separator and cathode binder for the assembly of all-polymer-based thin-film Li/coPIL/$LiFePO_4$ cells. Such lithium-metal battery prototypes were capable to work at 70°C and to deliver high specific capacity (up to 115 mAh/g) at medium C/15 current rate.

Key words: poly(ionic liquid)s, single-ion conductor, lithium battery, polymer electrolyte, solid state

1. INTRODUCTION:

The ever-growing need for more reliable and longer lasting lithium batteries motivates the research on new polymeric materials for energy storage applications [1]. State-of-the-art electrolytes for lithium batteries are based on mixtures of organic carbonates and various lithium salts. These liquid electrolytes allow for optimal battery operation under standard conditions. However, highly stressed operating conditions – namely excessive temperature or high current loads – may cause electrolyte decomposition, gas formation inside the device, ignition and ultimately catastrophic battery failures. Solid polymer electrolytes (SPEs) represent a safer alternative to conventional electrolytes [2,3]. SPEs offer high thermal stability, non-volatility, and high electrochemical stability. Additionally, the use of SPEs can avoid the risk of leaking of toxic, flammable and corrosive electrolytes and simplify the battery design, thus increasing energy density.

Starting from 1980-x the blends of a lithium salt and a polymer host have been extensively investigated as SPEs using various combinations of lithium salts in polymers [4]. Polyethylene oxide (PEO) is considered the golden standard among SPEs due to its ability for salts dissolution and the specific ion coordination properties of the ether groups [5]. The alternative approach to salt-in-polymer SPEs is to incorporate covalently lithium

salt moieties into the main polymer chain. These all-in-one electrolytes are formed by a main polymer chain carrying anionic functional groups and lithium ions as the mobile counterpart. The main advantage of the so-called "single-ion conductors" are (1) lithium transference number approaching unity and (2) no detrimental ion-concentration gradients during battery operation [6–8]. Nevertheless, single-ion conductors exhibit typically low room-temperature ionic conductivity which limits their use to high temperatures range application (> 50 ºC) [8].

A number of condensation synthetic routes have been employed to prepare single-ion conductors, such as polysiloxanes [6,9], polyepoxides [7,10,11], polyphosphazenes [12], poly(arylene ether)s [13,14] and polyurethanes [15]. However, the single-ion conductors based on (meth)acrylic and vinyl-type polymers have received broader interest due to simplicity of their preparation via radical polymerization and high tolerance of the later towards ionic functional groups [8,16]. The early reports on single ion conductors obtained via polymerization were mainly focused on monomers bearing strongly coordinating anions, such as: carboxylates [17,18], and sulfonates [19,20]. Further notable improvements in ionic conductivity were achieved after the introduction of weakly coordinating and highly delocalized anions, such as the sulfonamide group [21,22]. To further increase the conductivity anionic monomers can be copolymerized with neutral monomers. For instance, with monomers having flexible oxyethylene segments that can lower the glass transition temperature of the polymer and thus enhance the ionic conductivity of the polyelectrolyte [16]. However, the real breakthrough was achieved only with the synthesis of complex macromolecular architectures (block or triblock copolymers) via advanced polymerization methods such as reversible addition-fragmentation chain-transfer (RAFT) [23–25] or nitroxide-mediated polymerization (NMP) [26–29]. The comparison of the ionic conductivity in BAB triblock copolymers synthesized from two commonly used ionic monomers, namely lithium 1-[3-(methacryloyloxy)propylsulfonyl]-1-(trifluoromethylsulfonyl)imide (Scheme 1, **ILM5**) and lithium 4-styrenesulfonyl(trifluoromethylsulfonyl)imide (Scheme 1, **ILM6**), revealed the superiority of the methacrylic building block [27].

Although the obtained (multi)block copolymers showed promising results in terms of high ionic conductivity (up to 3×10^{-6} S/cm), high lithium transference number (>0.8) and satisfactory testing in Li batteries, the techniques used for their synthesis (RAFT and NMP) are considered as rather complicated and expensive for industrial application. Therefore, the implementation of a simple techniques such as free-radical polymerization

for the synthesis of polyelectrolytes with similar or superior properties is highly desired. Taking into account that the increase in molecular weight of poly(1-(3-(methacryloyloxy)propylsulfonyl)-1-(trifluoromethylsulfonyl)imide lithium) block is accompanied by the drop in ionic conductivity of polyelectrolyte owing to the rise of copolymer's T_g [23,27], the development of new ionic monomers with longer and more flexible spacers is required for the preparation of single-ion conductors by free radical polymerization.

In this work, we present the synthesis of four novel ionic liquid like methacrylic monomers differed by the structure and length of spacer (Scheme 1, **ILM1**-**ILM2** and **ILM3**-**ILM4**) and by the nature of chemically bonded anion (Scheme 1, **ILM1**, **ILM2** and **ILM3**-**ILM4**). Their free-radical copolymerization with poly(ethylene glycol) methyl ether methacrylate, varying the quantity of the later, afforded series of high molecular weight random copolymers showing low T_g (-62 – -27ºC) and ionic conductivity up to 1.9×10^{-6} S/cm at 25ºC. Finally, on the basis of polyelectrolyte with highest conductivity the lab-scale lithium cell prototypes were constructed and tested, thus demonstrating the promising prospects of the new single-ion conductors for the creation of truly solid Li batteries.

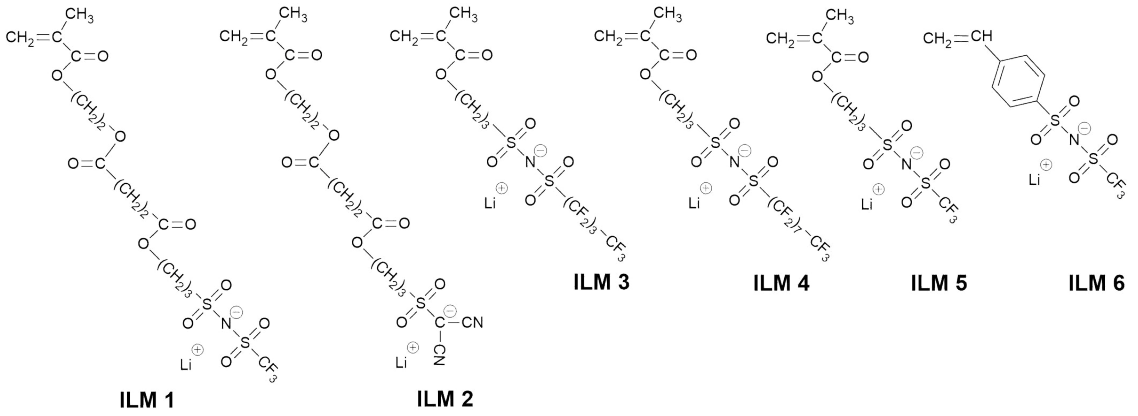

Scheme 1. Anionic monomers synthesized in the present study (**ILM1**-**ILM4**) and ILMs commonly used for the preparation of single ion conductors (**ILM5**-**ILM6**).

2. EXPERIMENTAL

2.1. Materials

Poly(ethylene glycol) methyl ether methacrylate (PEGM, M_w = 475 g/mol, Aldrich), 4-methoxyphenol (99%, Acros), 4-(2-(methacryloyloxy)ethoxy)-4-oxobutanoic acid (**1**, mono-2-(methacryloyloxy)ethyl succinate, 98%, Aldrich), 1,3-propane sultone (99%,

ABCR), lithium hydride (LiH, 97%, Sigma-Aldrich), perfluorobutanesulphonyl fluoride (ABCR, 95%), perfluorooctanesulfonyl fluoride (ABCR, 95%), methanol (Acros), hexane (Acros), dicloromethane (DCM, Acros), acetonitrile (ACN, HPLC grade 99%, Acros), dimethyl formamide (DMF, Acros), carbon-coated lithium iron phosphate ($LiFePO_4$, Advanced Lithium Electrochemistry Co. Ltd.), carbon black C_{65} (Timcal), carbon coated aluminum current collector (Showa Denko), lithium metal foil (Chemetall Foote Corporation) were used without further purification. The Spectra/Por 3 (Spectrumlabs) dialysis tubing with MWCO 3500 Dalton were used for polymer dialysis.

THF was purified by refluxing over the deep purple sodium-benzophenone complex. Thionyl chloride (>99%, Aldrich) was distilled over linseed oil. Malononitrile (99%, Acros) was distilled under reduced pressure (bp=145-150 °C/15 mm Hg). Trifluoromethanesulfonamide (97%, ABCR) was sublimed prior to use. 2,2'-Azobisisobutyronitrile (AIBN, initiator, 98%, Acros) was recrystallized from methanol before use. Potassium 3-(methacryloyloxy) propane-1-sulfonate (Sigma-Aldrich, 98%, Aldrich) was carefully dried under vacuum (<1 mm Hg) at 25 °C for 2 h prior to use.

Perfluorobutanesulphonamide and perfluorooctanesulfonamide were synthesized by the reaction of corresponding perfluorosylfonyl fluorides with liquid NH_3 at -78ºC, followed by the treatment with dioxane/HCl mixture and purification by sublimation in a full accordance with the previously published procedure [30].

2.2. Monomer synthesis

*Potassium 4-(2-(methacryloyloxy)ethoxy)-4-oxobutanoate (**2**)*

The solution of potassium carbonate (3.04 g, 22 mmol) in 10 mL of water was added dropwise to 10.13 g of **1** (44 mmol) stabilized with catalytic amount of 4-methoxyphenol under vigorous stirring at RT. After 30 min the water was stripped off at 25°C/30 mm Hg and the obtained solid mass was additionally dried at 25°C/1 mm Hg for 2 h. The residue was dissolved in 45 mL of anhydrous dichloromethane and the precipitate was filtered off. The collected solution was evaporated at 25°C/10 mm Hg and the residual wax-like product was dried at 30°C/1 mm Hg for 6 h. Yield: 10.37 g (88%).

*Potassium 3-((4-(2-(methacryloyloxy)ethoxy)-4-oxobutanoyl)oxy)propane-1-sulfonate (**3**)*

The solution of 1,3-propane sultone (5.10 g, 42 mmol) in 10 mL of anhydrous acetonitrile was added to the solution of **2** (10.18 g, 38 mmol) and 4-methoxyphenol (0.50 g, 4 mmol)

in 10 mL of anhydrous acetonitrile at RT under stirring in inert atmosphere. The reaction was heated under reflux and continued at 85°C for 2.5 h. After cooling down to RT the solution was precipitated in 150 mL of anhydrous diethyl ether. The resultant white powder was washed with diethyl ether (3×40 mL) and dried at 25°C/1 mm Hg for 24 h. Yield: 12.0 g (81%); ^{1}H NMR, 600.1 MHz, D_2O, δ ppm: 6.05 (s, 1H, C$\underline{H}_2$=C(CH_3)–), 5.67 (s, 1H, C$\underline{H}_2$=C(CH_3)–), 4.35-4.33 (m, 4H, OC$\underline{H}_2$C$\underline{H}_2$O), 4.13 (t, 2H, J=6.0 Hz, OC$\underline{H}_2CH_2CH_2$), 2.91-2.88 (m, 2H, C$\underline{H}_2$S), 2.64 (m, 4H, C$\underline{H}_2$COO), 2.03-1.99 (m, 2H, C$\underline{H}_2CH_2$S), 1.91 (s, 3H, C$\underline{H}_3$–C=); ^{13}C NMR, 150 MHz, D_2O, δ ppm: 174.6 (2C, $CH_2\underline{C}$=O), 169.2 (=C-$\underline{C}$=O), 135.6 (CH_2=$\underline{C}$), 127.2 ($\underline{C}H_2$=C), 63.7 (2C, C$\underline{H}_2$O), 47.7 (C$\underline{H}_2$S), 28.9 (2C, $\underline{C}H_2$CO), 23.7 (C$\underline{H}_2CH_2$S), 17.4 (C$\underline{H}_3$-C=); Calc. for $C_{13}H_{19}KO_9S$ (390.4): C, 39.99%; H, 4.91%; S, 8.21%; Found: C, 39.11%; H, 4.83%; S, 8.28%.

*3-(Chlorosulfonyl)propyl (2-(methacryloyloxy)ethyl) succinate (**4**)*

The **3** (11.72 g, 30.0 mmol) was suspended in 25 mL of anhydrous THF under inert atmosphere, whereupon 1.0 mL of DMF and 0.1 g of 4-methoxyphenol were added. After stirring for 15 minutes at RT an excess of the thionyl chloride (21.43 g, 180.1 mmol) was added dropwise and stirring was continued at RT for 24 h. The as obtained suspension was carefully poured into the ice-water (200 mL). The upper aqueous layer was decanted and the lower organic yellowish oily layer was diluted with dichloromethane (90 mL). The CH_2Cl_2 solution was washed with water (6×35 mL) and then dried over anhydrous magnesium sulfate. $MgSO_4$ was filtered off, the dichloromethane was gently evaporated at 25°C/15 mm Hg and the product in a form of colorless to light yellow oil was dried at 25°C/1 mm Hg for 6 h. Yield: 9.46 g (85%); ^{1}H NMR, 600.1 MHz, $CDCl_3$, δ ppm: 5.99 (s, 1H, C$\underline{H}_2$=C(CH_3)–), 5.48 (s, 1H, C$\underline{H}_2$=C(CH_3)–), 4.21 (m, 4H, OC$\underline{H}_2$C$\underline{H}_2$O), 4.15 (t, 2H, J=6.0 Hz, OC$\underline{H}_2CH_2CH_2$), 3.72 (m, 2H, C$\underline{H}_2$S), 2.53 (m, 4H, C$\underline{H}_2$COO), 2.25 (m, 2H, C$\underline{H}_2CH_2$S), 1.81 (s, 3H, C$\underline{H}_3$–C=); ^{13}C NMR, 100.6 MHz, $CDCl_3$, δ ppm: 171.6 ($CH_2\underline{C}$=O), 171.5 ($CH_2\underline{C}$=O), 167.0 (=C-$\underline{C}$=O), 135.5 (CH_2=$\underline{C}$), 125.7 ($\underline{C}H_2$=C), 62.1, 61.9, 61.6, 60.9 (3 C$\underline{H}_2$O, C$\underline{H}_2$S), 28.4 (2C, C$\underline{H}_2$CO), 23.7 (C$\underline{H}_2CH_2$S), 17.8 (C$\underline{H}_3$-C=); IR (KBr), cm^{-1}: 3111 (w), 2970 (m, νCH), 2926 (m, νCH), 1741 (vs, νC=O), 1634 (w, νC=C), 1379 (vs, $\nu_{as}SO_2$), 1324 (m), 1208 (s), 1162 (s, ν_sSO_2), 1061 (w), 1034 (w), 948 (w), 814 (w), 597 (m), 525 (m); Calc. for $C_{13}H_{19}ClO_8S$ (370.8): C, 42.11%; H, 5.17%; Cl, 9.56%; Found: C, 42.05%; H, 5.18%; Cl, 9.72%.

*3-[4-(2-(methacryloyloxy)ethoxy)-4-oxobutanoyl)oxy) propylsulfonyl]-1-(trifluoromethanesulfonyl)imide triethylammonium (**5**)*

The solution of **4** (27.92 g, 75 mmol) in 70 mL of anhydrous THF was added dropwise under inert atmosphere to the solution of trifluoromethanesulfonamide (11.23 g, 75 mmol) and triethylamine (16.80 g, 166 mmol) in 80 mL of anhydrous THF cooled to 0°C in the ice bath. The reaction mass was stirred for 20 minutes at 0°C, then was allowed to warm up to RT and stirring was continued during 3 h. The precipitate was filtered off, a catalytic amount of 4-methoxyphenol was added as inhibitor and the filtrate was evaporated under reduced pressure at temperature below 30°C. The residual light-brown oil was dissolved in 175 mL of dichloromethane and washed with distilled water (4×40 mL). The CH_2Cl_2 solution was dried over anhydrous $MgSO_4$, the magnesium sulfate was filtered off and dichloromethane was stripped off under the reduced pressure. The product was obtained as light brown transparent fluid oil, which was dried at 35°C/10 mm Hg for 1 h and finally at 60°C/1 mm Hg for 10 h. Yield: 32.55 g (74%); ^{1}H NMR, 400.1 MHz, $CDCl_3$, δ ppm: 7.58 (bs, 1H, H–N(C2H5)3), 5.96 (s, 1H, CH_2=C(CH_3)–), 5.46 (s, 1H, CH_2=C(CH_3)–), 4.18 (m, 4H, OCH_2–CH_2O), 4.05 (t, 2H, J=6.4 Hz, OCH_2–CH_2–CH_2S), 3.07 (m, 2H CH_2S + 6H HN(CH_2CH_3)$_3$), 2.50-2.46 (m, 4H, CO-CH_2-CH_2–CO), 2.04-1.99 (m, 2H, CH_2–CH_2S), 1.78 (s, 3H, =C–CH_3), 1.19 (t, 9H, J = 7.3 Hz, HN(CH_2CH_3)$_3$); ^{13}C NMR, 100.6 MHz, $CDCl_3$, δ ppm: 171.6 (CH_2–CO), 166.6 (=C–CO), 135.4 (CH_2=C), 122.6 (CH_2=C), 119.7 (q, J_{CF}= 323 Hz, CF_3), 62.2 (OCH_2–CH_2–CH_2S), 61.9 (OCH_2–CH_2O), 51.4 (CH_2S), 46.4 (HN(CH_2CH_3)$_3$), 28.4 (CH_2–COO), 23.2 (CH_2–CH_2S), 17.7 (=C–CH_3), 8.2 (HN(CH_2CH_3)$_3$); ^{19}F NMR, 376.5 MHz, $CDCl_3$, δ ppm: -79.4; IR (KBr), cm^{-1}: 3462 (w), 3089 (m), 2963 (m, νCH), 2822 (m, νCH), 2733 (m, νCH), 2681 (w, νCH), 1736 (vs, νC=O), 1638 (m, νC=C), 1503 (w), 1454 (m), 1401 (m), 1323 (vs, $\nu_{as}SO_2$), 1299 (s), 1273 (s, νCF), 1181 (vs, ν_sSO_2), 1122 (vs), 1056 (vs, νCF), 954 (m), 877 (w), 839 (w), 814 (m), 755 (w), 712 (w), 624 (m), 603 (m), 573 (m), 516 (m), 401 (w); Calc. for $C_{20}H_{35}F_3N_2O_{10}S_2$ (584.6): C, 41.09%; H, 6.03%; N, 4.79%; Found: C, 40.91%; H, 6.10%; N, 4.65%.

*Lithium 3-[4-(2-(methacryloyloxy)ethoxy)-4-oxobutanoyl)oxy) propylsulfonyl]-1-(trifluoromethanesulfonyl)imide (**ILM 1**)*

To the solution of 3-[4-(2-(methacryloyloxy)ethoxy)-4-oxobutanol)oxy) propylsulfonyl]-1-(trifluoromethanesulfonyl)imide triethylammonium **5a** (15.00 g, 26 mmol) in 200 mL of anhydrous THF the lithium hydride (0.61 g, 77 mmol) was added in 3-4 portions at

room temperature under vigorous stirring and inert atmosphere. The reaction mass was stirred at 30ºC for 2, whereupon it was filtered from unreacted LiH and concentrated at RT/15 mm Hg till the formation of caramel like viscous substance. The viscous mass was thoroughly washed with anhydrous dichloromethane (70-80 mL×5) under inert atmosphere with mechanical stirrer. The product in a form of colorless honey was dried at 35ºC/10 mm Hg and further on at 40ºC/1 mm Hg for 2-3 h. Yield: 8.7 g (69%); ^{1}H NMR, 400.1 MHz, acetone-d_6, δ ppm: 6.07 (s, 1H, C$\underline{H}_2$=C(CH$_3$)–), 5.65 (s, 1H, C$\underline{H}_2$=C(CH$_3$)–), 4.33 (m, 4H, OC$\underline{H}_2$–C$\underline{H}_2$O), 4.18 (m, 2H, OC$\underline{H}_2$–CH$_2$–CH$_2$S), 3.14 (m, 2H, C$\underline{H}_2$S), 2.63 (s, 4H, CO-C$\underline{H}_2$-C$\underline{H}_2$–CO), 2.10 (m, 2H, C$\underline{H}_2$–CH$_2$S), 1.90 (m, 3H, =C–C$\underline{H}_3$); ^{13}C NMR, 100.6 MHz, acetone-d_6, δ ppm: 173.7 (2C, CH$_2$–$\underline{C}$O), 168.3 (=C–$\underline{C}$O), 137.9 (CH$_2$=$\underline{C}$), 127.2 ($\underline{C}$H$_2$=C), 122.2 (q, J_{CF}= 323 Hz, CF$_3$), 64.4 (O$\underline{C}$H$_2$–CH$_2$–CH$_2$S), 64.2 & 63.9 (O$\underline{C}$H$_2$–$\underline{C}$H$_2$O), 53.4 ($\underline{C}$H$_2$S), 30.4 ($\underline{C}$H$_2$–COO), 25.5 ($\underline{C}$H$_2$–CH$_2$S), 19.3 (=C–$\underline{C}$H$_3$); ^{19}F NMR, 376.5 MHz, acetone-d_6, δ ppm: -79.1; IR (KBr), cm^{-1}: 3121 (m, νCH), 2964 (vs, νCH), 1720 (vs, νC=O), 1637 (m, νC=C), 1456 (m), 1413 (m), 1323 (vs, ν_{asSO2}), 1285 (s, νCF), 1191 (vs, ν_sSO$_2$), 1124 (vs), 1060 (vs, ν_{CF}), 956 (w), 879 (w), 817 (m), 756 (w), 714 (w), 626 (m), 603 (m), 576 (m), 517 (m); Calc. for C$_{14}$H$_{19}$NO$_{10}$F$_3$S$_2$Li (489.4): C, 34.36%; H, 3.91%; N, 2.86%; Found: C, 34.25%; H, 4.15%; N, 2.92%.

*Lithium 1,1-dicyano-[3-((4-(2-(methacryloyloxy)ethoxy)-4-oxobutanoyl)oxy) propylsulfonyl]methanide (**ILM 2**)*

Monomer **ILM2** was obtained similarly to the procedure listed above for the synthesis of **ILM1** with an exception of malonitrile utilization instead of trifluoromethanesulfonamide. Yield: 70%; ^{1}H NMR, 400.1 MHz, CDCl$_3$, δ ppm: 6.05 (s, 1H, C$\underline{H}_2$=C(CH$_3$)–), 5.54 (m, 1H, C$\underline{H}_2$=C(CH$_3$)–), 4.27 (m, 4H, OC$\underline{H}_2$–C$\underline{H}_2$O), 4.12 (t, 2H, J=6.4 Гц, OC$\underline{H}_2$–CH$_2$–CH$_2$S), 3.30 (m, 2H, C$\underline{H}_2$S), 2.57 (m, 4H, C$\underline{H}_2$–CO), 2.10 (m, 2H, C$\underline{H}_2$–CH$_2$S), 1.87 (s, 3H, =C–C$\underline{H}_3$); ^{13}C NMR, 100.6 MHz, CDCl$_3$, δ ppm: 171.8 (2C, CH$_2$–$\underline{C}$O), 166.9 (=C–$\underline{C}$O), 135.6 (CH$_2$=$\underline{C}$), 125.9 ($\underline{C}$H$_2$=C), 119.9 (C≡N), 62.6 (O$\underline{C}$H$_2$–CH$_2$–CH$_2$S), 62.2 & 62.1 (O$\underline{C}$H$_2$–$\underline{C}$H$_2$O), 54.1 ($\underline{C}$H$_2$S), 38.9 ($\underline{C}$-C≡N), 28.7 (2C, $\underline{C}$H$_2$–COO), 25.5 ($\underline{C}$H$_2$–CH$_2$S), 18.0 (=C–$\underline{C}$H$_3$); IR (KBr), cm^{-1}: 3034 (w, νCH), 2960 (m, νCH), 2726 (w, νCH), 2190 (vs, ν_sC≡N), 2161 (vs, ν_{as}C≡N), 1738 (vs, νC=O), 1636 (m, νC=C), 1512 (w), 1473(m), 1456 (m), 1401 (m), 1364 (m), 1305 (vs, ν_{as}SO$_2$), 1282 (s), 1159 (vs, ν_sSO$_2$), 1135 (vs), 1074 (m), 1034 (w), 945 (w), 784 (w), 658 (w), 585 (m), 572 (m); Calcd. for C$_{11}$H$_{11}$F$_9$LiNO$_6$S$_2$ (495.3): C, 26.68%; H, 2.24%; F, 34.52; Found: C, 26.45%; H, 2.31%; F, 34.15%.

*Lithium 1-[3-(methacryloyloxy)propyl)sulfonyl]-1-[(4,4,4,4,4,4,4,4,4-nonafluoro-4λ^{12}-buta-1,3-diyn-1-yl)sulfonyl]imide (**ILM3**)*

ILM3 was synthesized in accordance with the procedure published previously for **ILM5** [23] with an exception of $C_4F_9SO_2NH_2$ application instead of $CF_3SO_2NH_2$. Yield: 80%; mp = 164.3ºC (DSC); ^{1}H NMR, 400.1 MHz, DMSO-d6, δ ppm: 6.04 (s, 1H, C<u>H</u>$_2$=C(CH$_3$)–), 5.68 (s, 1H, C<u>H</u>$_2$=C(CH$_3$)–), 4.18 (t, 2H, J=6.4 Hz, CO–O–C<u>H</u>$_2$–), 3.08-3.04 (m, 2H,–C<u>H</u>$_2$–SO$_2$-N-), 2.06-1.98 (m, 2H, O–CH$_2$–<u>CH</u>$_2$–), 1.88 (s, 3H, CH$_2$=C(C<u>H</u>$_3$)–); ^{13}C NMR, 100.6 MHz, DMSO-d6, δ ppm: 166.4 (C=O), 135.8 (CH$_2$=<u>C</u>), 125.7 (<u>C</u>H$_2$=C), 62.7 (CO-O-<u>C</u>H$_2$), 51.5 (<u>C</u>H$_2$-S), 23.5 (CH$_2$-<u>C</u>H$_2$-CH$_2$-), 17.9 (<u>C</u>H$_3$); ^{19}F NMR, 376.5 MHz, DMSO-d6, δ ppm: -4.7, -37.2, -45.3, -50.0; IR (KBr), cm^{-1}: 3435 (m), 2979 (w, νCH), 2942 (w, νCH), 2854 (w, νCH), 1712 (s, νC=O), 1640 (m, νC=C), 1460 (m), 1332 (vs, ν_{as}SO$_2$), 1285 (s), 1234 (vs, νCF), 1170 (vs, ν_sSO$_2$), 1079 (s, νCF), 1014 (m), 948 (m), 838 (m), 797 (m), 690 (w), 649 (m), 619 (m), 588 (m), 517 (s), 478 (w); Calcd. for $C_{11}H_{11}F_9LiNO_6S_2$ (495.3): C, 26.68%; H, 2.24%; F, 34.52; Found: C, 26.52%; H, 2.29%; F, 34.15%.

*Lithium 1-[3-(methacryloyloxy)propyl)sulfonyl]-1-[(8,8,8,8,8,8,8,8,8,8,8,8,8,8,8,8,8-heptadecafluoro-8λ^{20}-octa-1,3,5,7-tetrayn-1-yl)sulfonyl)imide (**ILM4**)*

ILM4 was synthesized applying the procedure published previously for **ILM5** [23] with an exception of $C_8F_{17}SO_2NH_2$ utilization instead of $CF_3SO_2NH_2$. Yield: 78%; mp = 145.5ºC (DSC); ^{1}H NMR, 400.1 MHz, DMSO-d6, δ ppm: 6.03 (s, 1H, C<u>H</u>$_2$=C(CH$_3$)–), 5.66 (s, 1H, C<u>H</u>$_2$=C(CH$_3$)–), 4.18 (t, 2H, J=6.4 Hz, CO–O–C<u>H</u>$_2$–), 3.08-3.04 (m, 2H,–C<u>H</u>$_2$–SO$_2$-N-), 2.05-2.01 (m, 2H, O–CH$_2$–<u>CH</u>$_2$–), 1.87 (s, 3H, CH$_2$=C(C<u>H</u>$_3$)–); ^{13}C NMR, 100.6 MHz, DMSO-d6, δ ppm: 166.6 (C=O), 136.0 (CH$_2$=<u>C</u>), 125.8 (<u>C</u>H$_2$=C), 62.9 (CO-O-<u>C</u>H$_2$), 51.6 (<u>C</u>H$_2$-S), 23.7 (CH$_2$-<u>C</u>H$_2$-CH$_2$), 18.1 (<u>C</u>H$_3$); ^{19}F NMR, 376.5 MHz, DMSO-d6, δ ppm: -80.3, -112.8, -120.1, -121.1, -121.5, -121.8, -122.6, -125.9; IR (KBr), cm^{-1}: 3430 (m), 2923 (w, νCH), 2854 (w, νCH), 1714 (s, νC=O), 1641 (m, νC=C), 1460 (w), 1336 (vs, ν_{as}SO$_2$), 1281 (m), 1207 (vs, νCF), 1152 (vs, ν_sSO$_2$), 1079 (s, νCF), 1019 (w), 947 (m), 827 (m), 660 (w), 662 (m), 558 (m), 532 (m), 479 (w); Calcd. for $C_{15}H_{11}F_{17}LiNO_6S_2$ (695.3): C, 25.91%; H, 1.59%; F, 46.45; Found: C, 25.62%; H, 1.64%; F, 45.60%.

2.3. Polymer synthesis

The example is given for the synthesis of **coPIL1.6** copolymer with the composition of [ILM1]:[PEGM] = 1:7 by wt. **ILM1** (0.50 g, 1.0 mmol), poly(ethylene glycol) methyl ether methacrylate (PEGM, 3.50 g, 7.36 mmol), DMF (8.00 g) and AIBN (0.04 g, 1.0 wt.%) were gently mixed in a Schlenk flask at ambient temperature. After triple freeze-thaw-pump cycles the flask was filled with argon and heated to 60°C for 6 h. The resultant transparent highly viscous polymer solution was slightly diluted with water, dialyzed against 0.5M aq. LiCl and further with water for 3 days, whereupon it was freeze-dried. The polymer represented butter like soft material that was thoroughly dried at 60ºC/high vacuum for 24 h and finally stored in the argon filled glove box for 5 days prior to further investigation. Yield: 2.80 g (70%). Calcd. for $C_{168}H_{313}F_3LiNO_{83.5}S_2$ (3811.33): C, 52.94%; H, 8.28%; N, 0.37%; Found: C, 52.71%; H, 8.43%; N, 0.34%; $M_w = 4.16\times10^5$, $M_w/M_n = 4.93$ (GPC); T_g = -55ºC (DSC); $\sigma_{DC} = 1.9 \times 10^{-6}$ S/cm (25ºC).

2.4. Characterization

NMR spectra were recorded on AMX-400 and Avance II 500 MHz spectrometers (Bruker) at 25°C in the indicated deuterated solvents and are listed in ppm. The signal corresponding to the residual protons of the deuterated solvent was used as an internal standard for ^{1}H and ^{13}C NMR, while for ^{19}F NMR the $CHCl_2F$ was utilized as an external standard. IR spectra were acquired on a Nicolet Magna-750 Fourier IR-spectrometer using KBr pellets (128 scans, resolution is 2 cm^{-1}).

A LC-20AD gel permeation chromatograph (Shimadzu) was used to determine M_n, M_w and PDI of the triblock copolymers. The chromatograph was equipped with an integrated IR detector, a TSK-GEL® SuperA SuperAW5000 column and a SuperAW-L Guard column (Tosoh Bioscience). The eluent was a 0.1 M LiCl solution in mixture of water/ACN (4:1 v/v) and the flow rate was of 0.5 mL min^{-1} at 30ºC. Pullulan standards (Shodex P-82, $M_w = 5 - 800\times10^3$) were used to perform calibration.

Differential Scanning Calorimetry (DSC) experiments were performed on a Q100 differential calorimeter (TA Instruments) with a heating rate of 10 ºC min^{-1} in the range of -90 to 90 ºC. Glass transitions and melting temperatures were measured during the second heating cycle. ILMs and PILs samples were hermetically sealed in aluminum pans inside Ar filled glove-box. Thermal gravimetric analysis (TGA) was carried out in air on a Q50 model (TA Instruments) applying a heating rate of 5 ºC/min.

Ionic conductivity (σ) was determined by electrochemical impedance spectroscopy (EIS) with a VSP potentiostat/galvanostat (Bio-Logic Science Instruments, France). To avoid any influence of moisture/humidity on the conductivity of polyelectrolytes the latter were preliminary dried at 80ºC/1 mm Hg for 12 h in the B-585 oven (Buchi Glass Drying Oven, Switzerland) and were transferred under vacuum inside an argon-filled glovebox (MBRAUN MB-Labstar, H_2O and O_2 content <0.5 ppm). Soft polyelectrolytes were sandwiched between two stainless steel electrodes. The distance between the electrodes was kept equal to 500 μm using a Teflon spacer ring with the inner area of 0.38 cm^2. Symmetrical stainless steel/polyelectrolyte/stainless steel assembly was clamped into the 2032 coin cell and afterwards was taken out from glovebox. EIS experiments were carried by applying a 10 mV perturbation in the frequency range from 10^{-2} to 2×10^5 Hz and in a temperature range from 22 to 95 ºC. Temperature was controlled using the programmed M-53 oven (Binder, Germany), where cells were allowed to reach thermal equilibrium for at least 45 minutes before each test.

Cyclic voltammetry (CV) was used to determine the electrochemical stability window of the solid polymer electrolytes at 70 °C. A CHI600 electrochemical analyzer/workstation (CH Instruments) and ECCStd (EL-CELL) test cells were used to carry out the electrochemical characterization. The two-electrode cells were assembled by sandwiching copolymers between the working electrode and a metal lithium foil served as a reference and counter electrode simultaneously. Moisture contaminations were avoided by assembling the cells inside the Ar-filled glove-box. Stainless steel and copper disks were used as working electrodes during anodic and cathodic stability measurements, respectively. To evaluate anodic limits, potential sweeps were carried out between OCV and 5.5 V vs. Li^+/Li at a constant rate of 0.2 mV/s. To determine cathodic limits, potential sweeps were performed between OCV and -0.5 V vs. Li^+/Li at the same constant rate.

The lithium-ion transference number (t_{Li^+}) was determined at 70 °C in the Li/coPIL1.6/Li cell with total applied potential bias of 0.16 V (ΔV) in accordance to method, described by Evans and Vincent [31] and using the following equation:

$$t_{Li+} = \frac{I^s(\Delta V - I^o R_1^o)}{I^o(\Delta V - I^s R_1^s)} \quad (1)$$

, where t_{Li+} is the Li transference number, ΔV is the potential applied across the cell, $R_1°$ and R_1^s are the initial and steady-state resistances of the passivating layer, I° and I^s are the initial and steady-state currents.

2.5. Li cells assembly and testing

A composition of 60 wt.% of carbon coated $LiFePO_4$, 30 wt.% of **coPIL1.6** and 10 wt.% of carbon black was used for cathodes preparation. Firstly, powders of active material and carbon black were gently mixed in a hand mortar and, successively added to the 5 wt.% solution of coPIL1.7 in water upon stirring. The stirring was continued at r.t. for 1 h and the suspension was finally homogenized using an ultra-turrax mixer for one hour. The obtained aqueous slurry was casted onto a carbon coated aluminum current collector using a doctor-blade with a blade height of 300 μm. Water was removed by evaporation at ambient temperature and further drying at 80 °C/high vacuum overnight for 12 h in the B-585 oven (Buchi Glass Drying Oven, Switzerland) and were transferred under vacuum inside an argon-filled glovebox (MBRAUN MB-Labstar, H_2O and O_2 content <0.5 ppm). The obtained composite electrode film's thickness after drying was 50-60 μm.

The layer of **coPIL1.6** was applied manually directly on the surface of the composite cathode film (S = 1.15 cm^2) and was covered by a metal lithium disk (S = 0.78 cm^2). Lab-scale $LiFePO_4$/coPIL1.7/Li battery prototypes were then housed inside the ECC-Std cells (EL-cell). Cells were galvanostatically cycled at 70 °C with an ARBIN BT2000 battery tester. The current rates were calculated using the active mass loading of the composite cathode and the theoretical specific capacity of LiFePO4 (170 mAh/g) and were indicated as C/n rates where n denotes the number of hours to fully charge/discharge the cell. The cutoff potential limits were 2.5 –3.8 V. The temperature of the cell was controlled using an environmental simulation chamber MK-53 (Binder).

3. RESULTS AND DISCUSSION

As it was shown previously [16,8,32,23,24,26,33,27,34,25,35] one of the key factors for the successful assembly of all-polymer based solid Li batteries is the conductivity of both the separator (anionic PIL) and the electrodes. An ionic conductivity of 10^{-5} S/cm at 25ºC is considered nowadays as a necessary requirement for the polymer separator to set the work of the solid state battery at ambient temperature [8]. Among various approaches towards the development of novel anionic polyelectrolytes with high ionic conductivity can be the design of new anionic monomers differed by higher charge delocalization and Li ions mobility.

3.1 Monomer synthesis

Evidently, nobody is able to fully forecast and predict the complex influence of the monomer structure upon the resultant PIL's properties, its glass transition temperature and bulk conductivity in particular [16]. However, some general rules to gain better higher conductivity were elaborated as follow: 1) the main polymer chain needs to be flexible; 2) the ionic center is preferred to be placed on the end of the comb-like side chains; 3) the spacer between the main polymer chain and the attached anion should flexible and preferably include ethylene oxide fragments [8]. Keeping this in mind, three main ideas were applied for the design of monomers in the present work: the elongation of the spacer between methacrylic reactive group and chemically bonded anion (Scheme 1, **ILM1** and **ILM2**) in comparison with the previously developed **ILM5** [23]; the establishment of the cyanomethanide anion as the cheap substitution of expensive bis(trifluoromethylsulfonyl)imide (TFSI) one (Scheme 1, **ILM2**) and the introduction of side fluorinated chains for plasticization of the resultant polymers (Scheme 1, **ILM3** and **ILM4**).

A multistage synthetic procedure for the preparation of **ILM1** and **ILM2** monomers was developed (Scheme 2). During first step the commercially available 4-(2-(methacryloyloxy)ethoxy)-4-oxobutanoic acid **1** is neutralized with potassium carbonate. The potassium salt **2** is then reacted with 1,3-propane sultone in a polar solvent and as a result of the simultaneous ring opening and ion exchange reactions another potassium salt **3** is formed (Scheme 2). The successive treatment of **3** with an excess of thionyl chloride in the presence of catalytic amount of DMF provides the sulfonyl chloride **4**. The reaction of the later with trifluoromethanesulfonamide or malononitrile in the presence of triethylamine excess results in the formation of corresponding ammonium salts **5**. Finally, salts **5** are converted into **ILM1** and **ILM2** by the reaction with an excess of lithium hydride. The obtained **ILM1** and **ILM2** monomers represent highly viscous honey like colorless or light brown liquids, respectively.

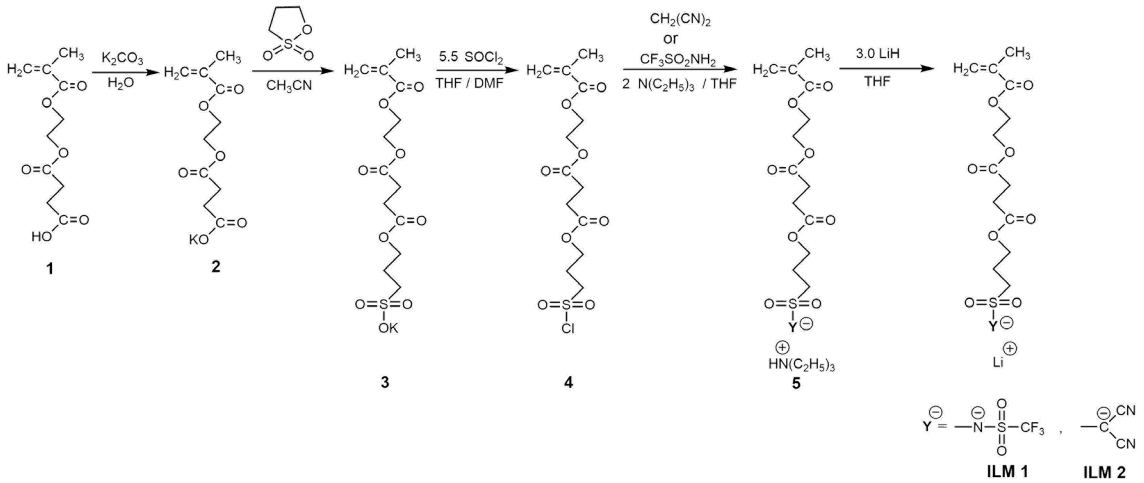

Scheme 2. Synthetic pathway for the preparation of **ILM1** and **ILM2**.

Monomers **ILM3** and **ILM4** were synthesized by analogy to **ILM1** and **ILM2**, however with some changes: the process started from the utilization of potassium 3-(methacryloyloxy) propane-1-sulfonate and the second step concludes in the reaction of sulfonyl chloride derivative with perfluorobutane or perfluorooctane sulfonamide (Scheme 3). After crystallization from the mixture of anhydrous THF/dichloromethane, **ILM3** and **ILM4** were isolated as white or white-beige crystalline powders with the melting points of 164.3 and 145.5ºC, respectively.

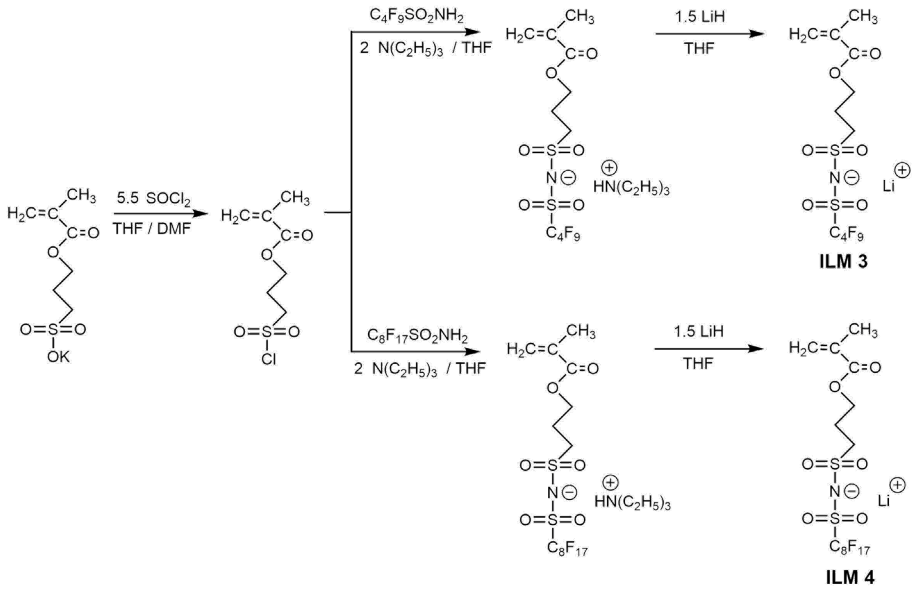

Scheme 3. Synthesis of **ILM3** and **ILM4**.

The structure and purity of **ILM1** – **ILM4** were proved by ^{1}H, ^{13}C and ^{19}F NMR, IR spectroscopy and elemental analysis. FTIR spectra of monomers show the absorption

bands at ~3120, 2990-2960, 2930-2920, 2880-2850 and 2720 cm^{-1} that are assigned to the CH_2 stretching. The absorption bands at 1710-1720 and 1630 cm^{-1} are identified as C=O vibrations of the ester and C=C bond, respectively. The characteristic bands of sulfonylimide anions were observed in **ILM1**, **ILM3** and **ILM4** at ~1320-1350 (asymmetric S=O), ~1180-1210 (CF), ~1120-1150 (symmetric S=O) and ~1050-1080 (CF) cm^{-1}, correspondingly. **ILM2** differs by the presence of bands at 2180 and 2160 cm^{-1} that are attributed to the vibration of the CN group in $-C^{-}(CN)_2$ anion. Although the ^{13}C NMR fully proves the structures of **ILM1** and **ILM2**, the signals from carbons of perfuorinated fragments in **ILM3** and **ILM4** were practically unresolvable. It can be explained by the fact, that due to the extensive C-F J-coupling and long range $^{13}C(-C)_n-^{19}F$ interactions, the signals underwent multiple splitting and thus appeared dissolved in the background noise. F^{19} NMR spectra of **ILM1** contains the singal signal of CF_3 group at -79.1 ppm, while for **ILM3** and **ILM4** a series of chemical shifts were observed in range of -4.7 ÷ -125.9 ppm.

3.2 Free radical copolymerization of ILM1-ILM4 and PEGM

At first the free radical homo polymerization of **ILM1** was carried out. The resultant polyelectrolyte possessed high molecular weight, shows T_g around RT and very low conductivity (Table 1, entry 1). Thus, **ILM1** was further copolymerized with poly(ethylene glycol) methyl ether methacrylate (PEGM) providing a set of copolymers differed in the ratio between **ILM1** and PEGM (Table 1, entries 2-8). PEGM was chosen due to the presence of oxyethylene fragments in its side chain that by analogy with PEO [36] should improve the solubility of ionic species, facilitate their dissociation, and promote an increase in the conductivity of the resultant copolymers. Free radical copolymerization performed in DMF with 1 wt.% of AIBN at 60°C and a concentration of 33 wt. % ([monomers]:[DMF]=1:2 by wt.) allowed for the preparation of polymers with moderate yields of 70-80%. By raising concentration to 50 wt.% it was possible to enhance the yield up to 90-95%, however, in parallel this was increasing the risk of unwanted cross-linking reactions and the formation of the insoluble gel. Vice versa, the decrease of concentration down to 25 wt.% allows to avoid cross-linking, but results in the lowering of both the yields and molecular masses.

Synthesized copolymers **coPIL1.1-coPIL1.7** were readily soluble in water, alcohols, acetone, acetonitrile, and amide type solvents (DMF, DMSO, DMAc). Their

structure, composition and purity were supported by IR spectroscopy and elemental analysis. FTIR spectra of copolymers show the absorption bands at 3153, 3109, 2960 and 2878 cm^{-1} assigned to CH_2 stretching. The characteristic absorption bands of ester bond and of $-SO_2-N-SO_2CF_3$ anion were observed respectively at 1730 (C=O) and 1351 (asymmetric S=O), 1180 (CF), 1108 (symmetric S=O), 1051 (CF) cm^{-1}. Finally, the absence of residual monomers was proved by the disappearance of the band at 1636 cm^{-1} (C=C).

Since the highest ionic conductivity was achieved for **coPIL1.6** (Table 1, entry 7 and see the discussions in 3.4.), other ionic monomers **ILM2**-**ILM4** were copolymerized with PEGM in the same [ILM]:[PEGM] molar ratio equal to 1:7.2 (Table 1, entries 9-11). Copolymers **coPIL2**-**coPIL4** demonstrated solubility similar to that of **coPIL1** and their structure and purity was also supported by IR spectroscopy and elemental analysis. The only difference found for **coPIL2** IR spectrum was the presence of characteristic absorption bands at 2185 and 2158 cm^{-1} attributed to the vibration of the CN groups.

The investigation of copolymers molar masses characteristics (M_w and M_w/M_n) via GPC resulted in high M_w values varying in the range of 3.44 - 6.36×10^5 g/mol. At this, molecular weights of copolymers obtained with the same [ILM]:[PEGM] molar ratio were practically identical (Table 1, entries 7, 9-10), while magnification of **ILM1** portion generally led to increase in M_w (Table 1, entries 2-7).

3.3 Thermal properties

The safety limits of lithium based cells are mainly determined by the thermal and electrochemical stability of the electrolyte. For instance, accidental overheating of the battery may cause decomposition reactions of the electrolyte followed by an uncontrolled temperature rise and catastrophic battery failure, such as flaming or explosions. This mechanism is usually referred as “thermal runaway” [37]. Thus, the determination of the temperature operation limits for PILs planned to be implied in the Li batteries is very important. The thermal degradation behavior of the copolymers was assessed via thermo-gravimetric analysis. The weight loss profile of all coPILs revealed a one-step degradation mechanism. As an example the TGA plot for **coPIL1.6** is shown in Figure 1. The average onset weight temperature for copolymers based on **ILM1** and **ILM2** was found to be 210°C, while for **coPIL3** and **coPIL4** it was lower and reached only 170°C. For instance, T_{onset} values of coPILs decrease following the order below with respect to the chemical structure of the ionic monomer:

T_{onset} coPIL1.6 (230ºC) > T_{onset} coPIL2 (210oC) > T_{onset} coPIL4 (175ºC) ≈ T_{onset} coPIL3 (170ºC)

Overall, obtained polymer electrolytes were thermally stable at least up to 170°C in air. Such result is particularly interesting for application in "safe" lithium batteries as the thermal stability of conventional liquid electrolytes usually lies around 140 ºC under inert atmosphere.

The glass transition temperatures of copolymers were determined by DSC (Table 1). It was found that the transition from **PIL1** (Table 1, entry 1) to **coPIL1.1-coPIL1.7** (Table 1, entries 2-8) leads to the significant decrease in T_g. Moreover, the higher was the content of PEGM or the ratio of EO/Li in copolymers composition, the lower was the observed T_g (Fig. 2b) with the lowest value of -55ºC. For **coPIL1.1-coPIL1.7** samples the heat resistance was found to be in between those of homo poly(ionic liquid) and of poly(PEGM) (Table 1, entries 1, 2-8 and 13). The T_g was also dependent on the ionic monomer's nature and for copolymers based on **ILM1-ILM4** with the same PEGM molar ratio the T_g values ranged from –61 °C to –55 °C in the following order:

T_g coPIL3 (-61ºC) ≈ T_g coPIL4 (-61ºC) < T_g coPIL1.6 (-55ºC) ≈ T_g coPIL2 (-53ºC)

It should be also mentioned that for **coPIL3** and **coPIL4** additional transition peaks were observed in DSC at -9ºC (Table 1, entries 10-11). They could be attributed to partial "defrosting" or melting of the side perfluorinated chains.

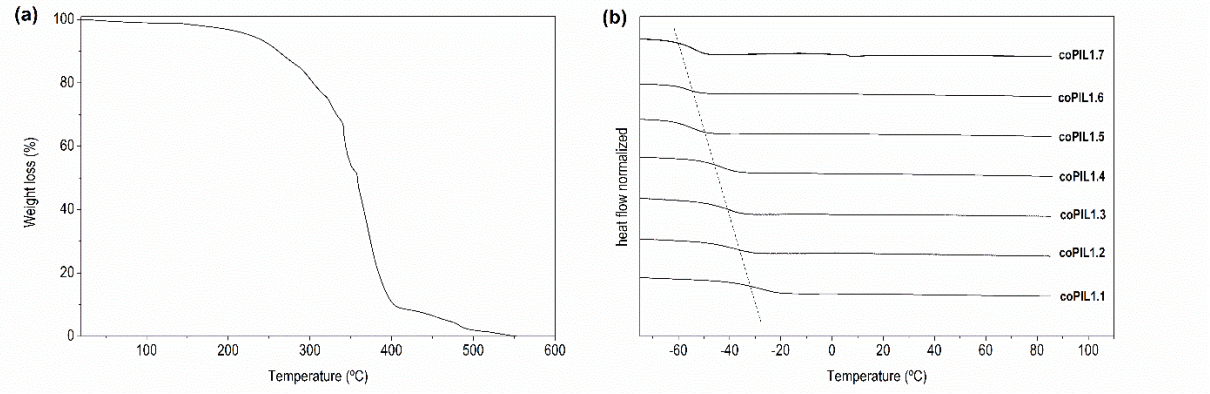

Fig. 1 TGA trace of **coPIL1.6** (a) and DSC traces for **coPIL1.1-coPIL1.7** copolymers of various ILM1/PEGM composition (b).

3.4. Ionic conductivity

Ionic conductivities of the polymer electrolytes were measured as a function of temperature by means of electrochemical impedance spectroscopy (EIS). At the beginning the conductivity of homo polymer, namely of **PIL1** was studied (Table 1, entry

1). Similarly to other anionic PILs with Li counter ions [21,23,32], polymerization of **ILM1** leads to the preparation of a solid material with the T_g around RT and very low conductivity (<10^{-11} S/cm at 25ºC). Although a longer and more flexible spacer was introduced in **ILM1**, the conductivity of **PIL1** in combination with Li cation was found to be nearly the same as for that reported previously for neat **PIL5** [23]. However, when **ILM1** was copolymerized with PEGM the observed conductivities began to differ by 4-5 orders of magnitude (Table 1, entries 2-8). Figure 2a shows the conductivity of **coPIL1.1**-**coPIL1.7** as a function of inverse temperature between 20 and 110ºC. As it can be seen, near room temperature, ionic conductivities varied between 10^{-7} and 10^{-6} S/cm and depending on the copolymers composition reached 10^{-5} S/cm at 50-80 ºC (Fig. 2a). The dependence of conductivity vs. temperature did not follow a linear Arrhenius behavior, indicating that lithium ions diffusion not only occurs as a hopping between the pending sulfonamide groups, but also resulted from local segmental motion of the coordination sites in the polymer main chain. In addition, a reciprocal relationship between ionic conductivity and glass transition temperature of copolymers was observed. At 25ºC ionic conductivities increased with decreasing the T_g, showing a maximum of 1.9×10^{-6} S/cm for **coPIL1.6**, i.e. for [EO]/[Li] ratio equal to 61. As it was shown before [16], by decreasing the T_g of a PIL it is possible to enhance the mobility of its chain's segments and since the movement of local polymer segments plays a role in the conduction of lithium ions, the decrease of T_g has a beneficial effect on σ. However, this effect is balanced by decreasing the concentration of lithium ions or, by other words, the charge carriers upon the increase in PEGM part, that eventually causes the ionic conductivity of **coPIL1.7** to fall in comparison with the others (Table 1, entries 8 and 2-7).

Keeping in mind that the highest conductivity was measured for **coPIL1.6**, **ILM2**-**ILM4** were copolymerized with PEGM in the same [EO]/[Li] ratio equal to 61 (Table 1, entries 9-11). Depending on the ionic monomer's nature the σ values determined at 25°C for the synthesized coPILs increase from 8.6×10^{-8} to 1.9×10^{-6} S/cm and can be ranked in the following decreasing order:

$$\sigma\ \text{coPIL1.6} >> \sigma\ \text{coPIL2} > \sigma\ \text{coPIL4} > \sigma\ \text{coPIL3}$$

It should also be mentioned that due to the specific structure of novel monomers, namely long and flexible spacer between methacrylic reactive group and chemically bonded anion (**ILM1** and **ILM2**) or plasticizing side perfluorinated chain (**ILM3** and **ILM4**), their copolymers with PEGM prepared by simple free radical polymerization

were able to show ionic conductivities comparable to that of **ILM5**/PEGM copolymers synthesized via more complicated RAFT process [23]. At this, the free radical polymerization copolymerization of **ILM5** with PEGM in the [EO]/[Li] ratio determined as optimal in this work, led to the preparation of **coPIL5** demonstrating lower conductivities than **coPIL1.6** and **coPIL2-coPIL4**. (Table 1, compare entry 12 and 7, 9-11).

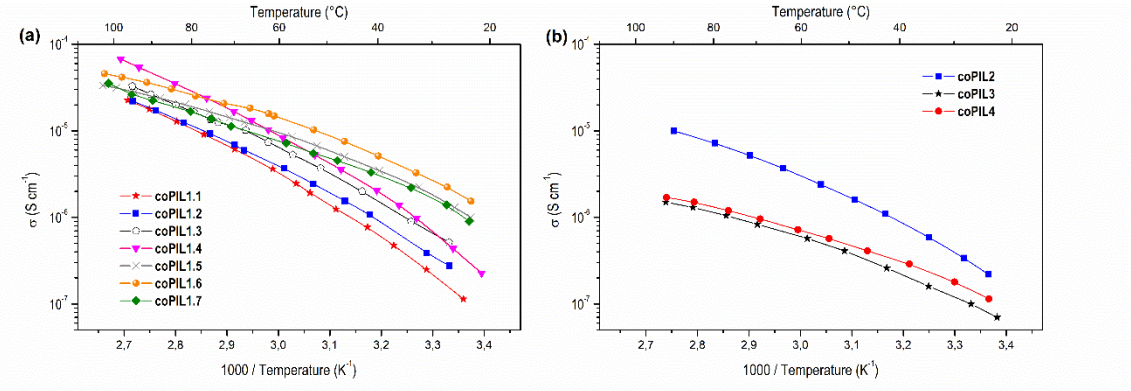

Fig. 2. Ionic conductivity vs temperature dependence for **coPIL1** copolymers of various ILM1/PEGM composition (a) and for **coPIL2-coPIL4** (b).

3.5. Electrochemical stability

The electrochemical stability limits of the copolymers were assessed via cyclic voltammetry. Figure 3 shows the anodic and cathodic scans of **coPIL1-coPIL4** at 70 ºC. Figure **3a** demonstrates the cathodic scan of **coPIL1.6** against an inert copper electrode. Moving towards more negative potentials a rise in the cathodic current was observed between 0 and - 0.5 V *vs.* Li^+/Li, followed by a wave between -0.5 and 0.35 V *vs.* Li^+/Li. This process is attributed with lithium plating and stripping at the electrode surface. A couple of peaks are observed at 0.68 and 0.86 *vs.* Li^+/Li and can be ascribed to redox process of electrode active species, such as oxides [38]. The oxidation potential for **coPIL1.6** against a SS electrode was found at 4.2 V *vs.* Li^+/Li, as indicated by the sudden rise in the anodic current (Fig. 3a). The CV of **coPIL2-coPIL4** performed in a similar conditions demonstrates the anodic limit at 4.0, 4.4 and 4.6 V *vs.* Li^+/Li, respectively. Thus, the overall evolution of electrochemical stability of coPILs can be summarized as follows:

ESW coPIL4 > ESW coPIL3 > ESW coPIL1 > ESW coPIL2

The electrochemical stability towards oxidative processes at the interface with the cathode is particularly important for battery application. This experiment demonstrates that the coPILs synthesized in this work are anodically stable at the operating voltage of common cathodes for LIBs, such as $LiFePO_4$ and $LiCoO_2$. At this, the TFSI-like anions show higher electrochemical stability than that based on 1,1-dicyano methanide (Fig. 3).

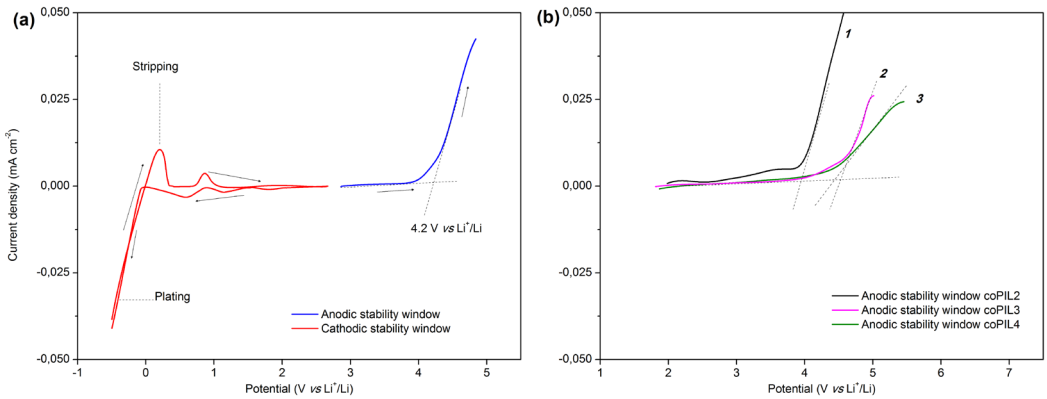

Fig. 3. Electrochemical stability window (ESW) for **coPIL1.6** (a), **coPIL2** (b, line 1), **coPIL3** (b, line 2) and **coPIL4** (b, line 3) at 70 ºC (stainless steel as the working electrode and Li foil as the counter and reference electrodes, scan rate 0.2 mV s^{-1}).

3.6. Lithium-ion transference number

The lithium-ion transference number for **coPIL1.6** showing highest ionic conductivity was evaluated at 70°C using the method of Vincent and Evans [31]. The test was performed by assembling the Li/coPIL1.6/Li cell and study of its properties before and after the polarization experiment (Fig. S1-S3, see the ESI file). Applying the Z fit program to the Nyquist plots of a.c. impedance of a Li/coPIL1.6/Li cell at 70°C it was possible to determine the initial and steady-state resistances equal to 5346 and 10175 Ω, respectively (Fig. S2 and S3). The study of current's response during polarization of the cell (Fig. S1) provided the change from 0.014 to 0.0095 mA. Further, by applying an equation (1), the lithium transference number as high as 0.91 was calculated. Such high t_{Li+} can be explained by the fact that, while negative charges are chemically bonded to polymer chain, the lithium cations are the only species free to move and, thus the only species responsible for ionic conductivity.

3.7. Lab-scale solid-state Li-cells testing

Finally, to further confirm the significance of the newly prepared polymer single ion conductors, the lab-scale lithium cell prototypes based on **coPIL1.6** with highest ionic

conductivity were assembled using a lithium-metal negative electrode and a carbon-coated $LiFePO_4$ as a model active material for the positive electrode. The cathode for the Li/coPIL1.6/$LiFePO_4$ cells was composed of 60 wt.% $LiFePO_4$, 30 wt.% **coPIL1.6**, and 10 wt.% carbon black. The assembled Li/coPIL1.6/$LiFePO_4$ battery was tested at 70 ºC (Fig. 4). Cycling tests were conducted at different current rates, where the rate is denoted as C/n corresponding to a full discharge or full charge of the theoretical cathode capacity (C) in n hours. At C/15 rate the all-polymer cell was able to deliver an average specific capacity of 115 mAh/g. When the current was increased to C/10 the capacity dropped down to 100 mAh/g, while at C/5 the delivered specific capacity was around 40 mAh/g. Although a decrease in capacity was observed after some cycles, the cell was capable to reversibly charge/discharge at least up to 90 cycles (Fig. 4). The charge/discharge efficiency was found to exceed 95% upon initial cycling (>99% at C/10), confirming a good reversibility of the lithium ion intercalation process as well as the electrochemical stability of prepared copolymer electrolytes.

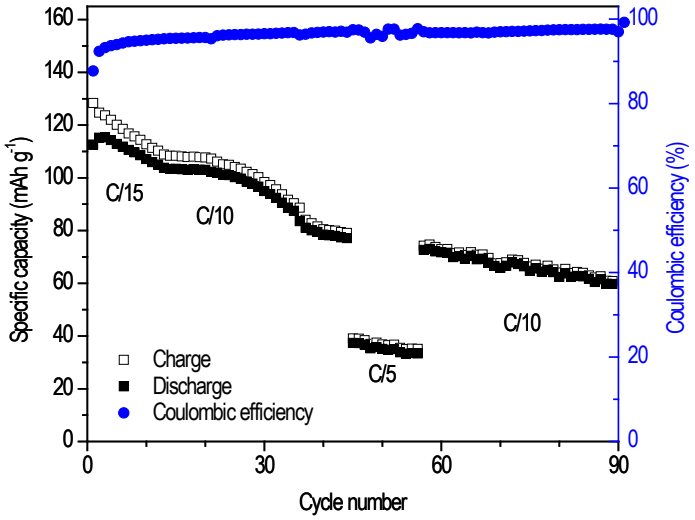

Fig. 4. Specific capacity and coulombic efficiency versus cycle number profile of the Li/coPIL1.6/$LiFePO_4$ cell at different charge / discharge rates at 70 ºC.

4. CONCLUSIONS

In summary, four novel ionic liquid like monomers have been designed and synthesized in high purity. Due to the specific structure of novel monomers, namely long and flexible spacer between methacrylic reactive group and chemically bonded anion (**ILM1** and **ILM2**) or plasticizing side perfluorinated chain (**ILM3** and **ILM4**), their

copolymers with poly(ethylene glycol) methyl ether methacrylate (PEGM) prepared via simple free radical polymerization were able to show low T_g (-61 ÷ -27°C) and high ionic conductivities (up to 10^{-6} S/cm at 25°C).

By investigation of **ILM1**/PEGM copolymerization and detailed characterization of obtained polyelectrolytes it was possible to identify the impact of the copolymer composition on thermal and ion conducting properties. It was found that the highest ionic conductivity is demonstrated by the copolymer synthesized at [EO]/[Li] ratio equal to 61. Tacking this ratio as optimal, the copolymerization of PEGM with other ionic monomers (**ILM2**-**ILM4**) was carried out. The comparison of ionic conductivity for copolymers revealed that the highest one is demonstrated by single ion conductor based on **ILM1**. The later was further suggested and tested as separator in all-polymer-based thin-film Li/coPIL1.6/$LiFePO_4$ lithium cells.

The most striking advantages of the suggested approach are summarized as follow: (1) the possibility to prepare polyelectrolytes via easy free radical (co)polymerization; (2) the ability to control both the T_g and ionic conductivity of copolymers simply varying the ILM/PEGM ratio; (3) the synthesis of solid polyelectrolytes with low T_g (up to −61 °C) and comparatively high σ in anhydrous state (up to 1.9×10^{-6} and 2×10^{-5} S/cm at 25 and 70 °C, respectively); (4) the preparation of single ion conductors with high lithium transference number (0.91) and high electrochemical stability (4.0-4.6 V vs Li^+/Li); (5) the assembly of solid-state lithium-metal battery prototypes capable to deliver comparably large capacities (up to 115 mAh/g) and to reversibly operate at medium current rates (up to C/5).

Acknowledgments

This work was supported by the grant of President of the Russian Federation ‘‘For Young Outstanding Professors” (project no. MD-2371.2017.3) and by European Commission (project no. 318873 «IONRUN»). L.P gratefully acknowledges financial support of the European Commission through project RENAISSANCE-ITN 289347.

References

[1] T. Placke, R. Kloepsch, S. Dühnen, M. Winter, Lithium ion, lithium metal, and alternative rechargeable battery technologies: the odyssey for high energy density, J. Solid State Electrochem. 21 (2017) 1939–1964. doi:10.1007/s10008-017-3610-7.

[2] A. Manuel Stephan, Review on gel polymer electrolytes for lithium batteries, Eur. Polym. J. 42 (2006) 21–42. doi:10.1016/j.eurpolymj.2005.09.017.

[3] V. Di Noto, S. Lavina, G.A. Giffin, E. Negro, B. Scrosati, Polymer electrolytes: Present, past and future, Electrochimica Acta. 57 (2011) 4–13. doi:10.1016/j.electacta.2011.08.048.
[4] A. Bouridah, F. Dalard, D. Deroo, M.B. Armand, Potentiometric measurements of ionic mobilities in poly(ethyleneoxide) electrolytes, Solid State Ion. 18–19, Part 1 (1986) 287–290. doi:10.1016/0167-2738(86)90128-1.
[5] K.E. Thomas, S.E. Sloop, J.B. Kerr, J. Newman, Comparison of lithium-polymer cell performance with unity and nonunity transference numbers, J. Power Sources. 89 (2000) 132–138. doi:10.1016/S0378-7753(00)00420-1.
[6] S. Liang, U.H. Choi, W. Liu, J. Runt, R.H. Colby, Synthesis and Lithium Ion Conduction of Polysiloxane Single-Ion Conductors Containing Novel Weak-Binding Borates, Chem. Mater. 24 (2012) 2316–2323. doi:10.1021/cm3005387.
[7] K. Matsumoto, T. Endo, Preparation and properties of ionic-liquid-containing poly(ethylene glycol)-based networked polymer films having lithium salt structures, J. Polym. Sci. Part Polym. Chem. 49 (2011) 3582–3587. doi:10.1002/pola.24795.
[8] H. Zhang, C. Li, M. Piszcz, E. Coya, T. Rojo, L.M. Rodriguez-Martinez, M. Armand, Z. Zhou, Single lithium-ion conducting solid polymer electrolytes: advances and perspectives, Chem. Soc. Rev. 46 (2017) 797–815. doi:10.1039/C6CS00491A.
[9] C. Ren, M. Liu, J. Zhang, Q. Zhang, X. Zhan, F. Chen, Solid-state single-ion conducting comb-like siloxane copolymer electrolyte with improved conductivity and electrochemical window for lithium batteries, J. Appl. Polym. Sci. 135 (2018) n/a-n/a. doi:10.1002/app.45848.
[10] K. Matsumoto, T. Endo, Synthesis of networked polymers with lithium counter cations from a difunctional epoxide containing poly(ethylene glycol) and an epoxide monomer carrying a lithium sulfonate salt moiety, J. Polym. Sci. Part Polym. Chem. 48 (2010) 3113–3118. doi:10.1002/pola.24092.
[11] K. Matsumoto, T. Endo, Synthesis of networked polymers by copolymerization of monoepoxy-substituted lithium sulfonylimide and diepoxy-substituted poly(ethylene glycol), and their properties, J. Polym. Sci. Part Polym. Chem. 49 (2011) 1874–1880. doi:10.1002/pola.24614.
[12] H.R. Allcock, D.T. Welna, A.E. Maher, Single ion conductors—polyphosphazenes with sulfonimide functional groups, Solid State Ion. 177 (2006) 741–747. doi:10.1016/j.ssi.2006.01.039.
[13] H. Oh, K. Xu, H.D. Yoo, D.S. Kim, C. Chanthad, G. Yang, J. Jin, I.A. Ayhan, S.M. Oh, Q. Wang, Poly(arylene ether)-Based Single-Ion Conductors for Lithium-Ion Batteries, Chem. Mater. 28 (2016) 188–196. doi:10.1021/acs.chemmater.5b03735.
[14] Y. Chen, H. Ke, D. Zeng, Y. Zhang, Y. Sun, H. Cheng, Superior polymer backbone with poly(arylene ether) over polyamide for single ion conducting polymer electrolytes, J. Membr. Sci. 525 (2017) 349–358. doi:10.1016/j.memsci.2016.12.011.
[15] L. Porcarelli, K. Manojkumar, H. Sardon, O. Llorente, A.S. Shaplov, K. Vijayakrishna, C. Gerbaldi, D. Mecerreyes, Single Ion Conducting Polymer Electrolytes Based On Versatile Polyurethanes, Electrochimica Acta. 241 (2017) 526–534. doi:10.1016/j.electacta.2017.04.132.
[16] A.S. Shaplov, R. Marcilla, D. Mecerreyes, Recent Advances in Innovative Polymer Electrolytes based on Poly(ionic liquid)s, Electrochim Acta. 175 (2015) 18–34. doi:10.1016/j.electacta.2015.03.038.
[17] N. Kobayashi, M. Uchiyama, E. Tsuchida, Poly[lithium methacrylate-co-oligo(oxyethylene)methacrylate] as a solid electrolyte with high ionic conductivity, Solid State Ion. 17 (1985) 307–311. doi:10.1016/0167-2738(85)90075-X.
[18] S.-W. Ryu, P.E. Trapa, S.C. Olugebefola, J.A. Gonzalez-Leon, D.R. Sadoway,

A.M. Mayes, Effect of Counter Ion Placement on Conductivity in Single-Ion Conducting Block Copolymer Electrolytes, J. Electrochem. Soc. 152 (2005) A158–A163. doi:10.1149/1.1828244.
[19] C.H. Park, Y.-K. Sun, D.-W. Kim, Blended polymer electrolytes based on poly(lithium 4-styrene sulfonate) for the rechargeable lithium polymer batteries, Electrochimica Acta. 50 (2004) 375–378. doi:10.1016/j.electacta.2004.01.110.
[20] X.-G. Sun, J. Hou, J.B. Kerr, Comb-shaped single ion conductors based on polyacrylate ethers and lithium alkyl sulfonate, Electrochimica Acta. 50 (2005) 1139–1147. doi:10.1016/j.electacta.2004.08.011.
[21] R. Meziane, J.-P. Bonnet, M. Courty, K. Djellab, M. Armand, Single-ion polymer electrolytes based on a delocalized polyanion for lithium batteries, Electrochimica Acta. 57 (2011) 14–19. doi:10.1016/j.electacta.2011.03.074.
[22] A.S. Shaplov, P.S. Vlasov, M. Armand, E.I. Lozinskaya, D.O. Ponkratov, I.A. Malyshkina, F. Vidal, O.V. Okatova, G.M. Pavlov, C. Wandrey, I.A. Godovikov, Y.S. Vygodskii, Design and synthesis of new anionic "polymeric ionic liquids" with high charge delocalization, Polym Chem. 2 (2011) 2609–2618. doi:10.1039/C1PY00282A.
[23] L. Porcarelli, A.S. Shaplov, M. Salsamendi, J.R. Nair, Y.S. Vygodskii, D. Mecerreyes, C. Gerbaldi, Single-Ion Block Copoly(ionic liquid)s as Electrolytes for All-Solid State Lithium Batteries, ACS Appl. Mater. Interfaces. 8 (2016) 10350–10359. doi:10.1021/acsami.6b01973.
[24] L. Porcarelli, M.A. Aboudzadeh, L. Rubatat, J.R. Nair, A.S. Shaplov, C. Gerbaldi, D. Mecerreyes, Single-ion triblock copolymer electrolytes based on poly(ethylene oxide) and methacrylic sulfonamide blocks for lithium metal batteries, J. Power Sources. 364 (2017) 191–199. doi:10.1016/j.jpowsour.2017.08.023.
[25] C. Jangu, A.M. Savage, Z. Zhang, A.R. Schultz, L.A. Madsen, F.L. Beyer, T.E. Long, Sulfonimide-Containing Triblock Copolymers for Improved Conductivity and Mechanical Performance, Macromolecules. 48 (2015) 4520–4528. doi:10.1021/acs.macromol.5b01009.
[26] R. Bouchet, S. Maria, R. Meziane, A. Aboulaich, L. Lienafa, J.-P. Bonnet, T.N.T. Phan, D. Bertin, D. Gigmes, D. Devaux, R. Denoyel, M. Armand, Single-ion BAB triblock copolymers as highly efficient electrolytes for lithium-metal batteries, Nat. Mater. 12 (2013) 452–457. doi:10.1038/nmat3602.
[27] D. Devaux, L. Liénafa, E. Beaudoin, S. Maria, T.N.T. Phan, D. Gigmes, E. Giroud, P. Davidson, R. Bouchet, Comparison of single-ion-conductor block-copolymer electrolytes with Polystyrene- TFSI and Polymethacrylate- TFSI structural blocks, Electrochimica Acta. 269 (2018) 250–261. doi:10.1016/j.electacta.2018.02.142.
[28] T.N.T. Phan, A. Ferrand, H.T. Ho, L. Liénafa, M. Rollet, S. Maria, R. Bouchet, D. Gigmes, Vinyl monomers bearing a sulfonyl(trifluoromethane sulfonyl) imide group: synthesis and polymerization using nitroxide-mediated polymerization, Polym. Chem. 7 (2016) 6901–6910. doi:10.1039/C6PY01004K.
[29] I. Villaluenga, S. Inceoglu, X. Jiang, X.C. Chen, M. Chintapalli, D.R. Wang, D. Devaux, N.P. Balsara, Nanostructured Single-Ion-Conducting Hybrid Electrolytes Based on Salty Nanoparticles and Block Copolymers, Macromolecules. 50 (2017) 1998–2005. doi:10.1021/acs.macromol.6b02522.
[30] J. Foropoulos, D.D. DesMarteau, Synthesis, properties, and reactions of bis((trifluoromethyl)sulfonyl) imide, (CF3SO2)2NH, Inorg. Chem. 23 (1984) 3720–3723. doi:10.1021/ic00191a011.
[31] J. Evans, C.A. Vincent, P.G. Bruce, Electrochemical measurement of transference numbers in polymer electrolytes, Polymer. 28 (1987) 2324–2328. doi:10.1016/0032-3861(87)90394-6.

[32] L. Porcarelli, A.S. Shaplov, F. Bella, J.R. Nair, D. Mecerreyes, C. Gerbaldi, Single-Ion Conducting Polymer Electrolytes for Lithium Metal Polymer Batteries that Operate at Ambient Temperature, ACS Energy Lett. (2016) 678–682. doi:10.1021/acsenergylett.6b00216.
[33] D. Devaux, D. Glé, T.N.T. Phan, D. Gigmes, E. Giroud, M. Deschamps, R. Denoyel, R. Bouchet, Optimization of Block Copolymer Electrolytes for Lithium Metal Batteries, Chem. Mater. 27 (2015) 4682–4692. doi:10.1021/acs.chemmater.5b01273.
[34] O. Green, S. Grubjesic, S. Lee, M.A. Firestone, The Design of Polymeric Ionic Liquids for the Preparation of Functional Materials, Polym. Rev. 49 (2009) 339–360. doi:10.1080/15583720903291116.
[35] Q. Ma, H. Zhang, C. Zhou, L. Zheng, P. Cheng, J. Nie, W. Feng, Y.-S. Hu, H. Li, X. Huang, L. Chen, M. Armand, Z. Zhou, Single Lithium-Ion Conducting Polymer Electrolytes Based on a Super-Delocalized Polyanion, Angew. Chem. Int. Ed. 55 (2016) 2521–2525. doi:10.1002/anie.201509299.
[36] T. Eschen, J. Kösters, M. Schönhoff, N.A. Stolwijk, Ionic Transport in Polymer Electrolytes Based on PEO and the PMImI Ionic Liquid: Effects of Salt Concentration and Iodine Addition, J. Phys. Chem. B. 116 (2012) 8290–8298. doi:10.1021/jp303579b.
[37] K. Xu, Nonaqueous Liquid Electrolytes for Lithium-Based Rechargeable Batteries, Chem. Rev. 104 (2004) 4303–4418. doi:10.1021/cr030203g.
[38] K.M. Abraham, Z. Jiang, B. Carroll, Highly Conductive PEO-like Polymer Electrolytes, Chem. Mater. 9 (1997) 1978–1988. doi:10.1021/cm970075a.

Table 1. Selected PIL's and random coPILs properties

No	Polyelect-rolyte	[ILM]/[PEGM] (wt. ratio)	[EO]/[Li]	$M_w \times 10^{-5}$ (g/mol)[a]	PDI[a]	T_g (°C)[b]	T_{onset} (°C)[c]	σ at 25 °C (S/cm)	Electrochemical window, (V)[d]
1	**PIL1**	-	-	10.50	3.11	18	225	$< 10^{-11}$	-
2	**coPIL1.1**	1:2	18	6.36	4.80	-27	230	1.2×10^{-7}	-
3	**coPIL1.2**	1:3	26	6.22	4.61	-37	230	2.3×10^{-7}	-
4	**coPIL1.3**	1:4	35	6.06	5.24	-40	230	3.7×10^{-7}	-
5	**coPIL1.4**	1:5	44	5.70	4.90	-43	235	4.1×10^{-7}	-
6	**coPIL1.5**	1:6	53	5.90	5.24	-55	230	1.2×10^{-6}	-
7	**coPIL1.6**	1:7	61	4.16	4.93	-55	230	1.9×10^{-6}	4.2
8	**coPIL1.7**	1:8	70	5.73	5.04	-55	230	1.1×10^{-6}	-
9	**coPIL2**	1:8.4	61	4.08	4.64	-53	210	2.5×10^{-7}	4.0
10	**coPIL3**	1:5.6	61	4.00	4.19	-61 (-9.2)[e]	170	8.6×10^{-8}	4.6
11	**coPIL4**	1:4.9	61	3.44	3.54	-61 (-9.3)[e]	175	1.3×10^{-7}	4.4
12[f]	**coPIL5**	1:9.9	61	4.57	4.35	-57	180	6.3×10^{-8}	4.3
13[f]	poly(**PEGM**)	-	∞	0.94	2.22	-62	160	-	-

[a]By GPC in 0.1 M LiCl solution of water/ACN (4:1 v/v) at 30ºC with pullulan standards calibration.

[b]By DSC.

[c]By TGA.

[d]Determined by cyclic voltammetry at 70ºC (stainless steel as the working electrode and Li foil as the counter and reference electrodes, scan rate 0.2 mV/s).

[e]T_m.

[f]For comparison.